

PACS numbers: 42.30.Wb; 42.62.Be
DOI: 10.1070/QE2002v032n11ABEH002334

Combined application of optical methods to increase the information content of optical coherent tomography in diagnostics of neoplastic processes

R.V. Kuranov, V.V. Sapozhnikova, N.M. Shakhova,
V.M. Gelikonov, E.V. Zagainova, S.A. Petrova

Abstract. **A combined application of optical methods [optical coherent tomography (OCT), cross-polarisation optical coherent tomography, and fluorescence spectroscopy] is proposed for obtaining information on morphological and biochemical changes occurring in tissues in norm and pathology. It is shown that neoplastic and scar changes in esophagus can be distinguished using a combination of polarisation and standard OCT due to the difference between the depolarising properties of the tissues caused by the structural properties of collagenic fibres in stroma. It is shown that OCT combined with fluorescence spectroscopy with the use of 5-aminolevulinic acid is promising for determining the boundaries of carcinoma of the uterine cervix and vulva. It is found that the tumour boundary detected by optical methods coincides with the morphological boundary and extends beyond colposcopically determined boundary by about 2 mm.**

Keywords: *optical coherent tomography, cross-polarisation optical coherent tomography, fluorescence spectroscopy, aminolevulinic acid.*

1. Introduction

At present the optical methods are finding increasing applications for the early diagnostics of neoplastic processes in tissues and many other pathologies [1 – 4]. The method of optical coherent tomography (OCT) is one of the promising noninvasive methods of the early diagnostics of structural disorders caused by pathological processes [5 – 7]. Physical measurements in OCT are based on interferometry with the use of broadband radiation sources in the visible or near-IR spectral ranges. Biological tissues, which are turbid media, weakly absorb radiation in the near-IR range between 0.83 and 1.3 μm but strongly scatter it. The temporal selection of a non-scattered or weakly scattered component of probe radiation in an optical coherent tomograph is used to obtain information on the optical inhomogeneities of a medium under study. OCT provides two-dimensional images (tomograms) of tissues with a resolution of 10 – 20 μm and allows the visualisation of the inner structure of ground tissues at a depth of up to 1 – 2 mm. The versatility and compactness of an optical tomograph equipped with endoscopic probes make is possible to use it for *in vivo* diagnostics of all ground tissues of human beings.

Analysis of the data on clinical applications of OCT showed that different morphological structures and tissue layers have different optical characteristics, which are determined by their spatial structure and refractive indices [8 – 10]. Healthy tissues are visualised in tomograms as layers with distinct boundaries. Because the scattering properties of epithelium and fibrous connective tissues are different, OCT is capable of displaying the layer-to-layer architectonics of healthy ground tissues.

It is known that small spherical particles (intracellular structures) and thin long components (fibres) strongly scatter radiation. Strong scattering of incident radiation is also inherent in cancerous and other metabolic cells, which are characterised by a high nuclear-cytoplasmic ratio, have a thickened membrane and contain many small intracellular organelles [11]. Light is scattered weaker in cellular cytoplasm and almost is not scattered in the intracellular liquid and inside blood vessels. By using these properties, we can perform the OCT diagnostics of pathologic processes proceeding in tissues, which change the characteristics of scattering.

However, sometimes it is difficult to distinguish by the OCT method the substantially different states, such as necrosis, cancer, papillomatous, and scar disorders, which have similar tomographic images preventing diagnostics. At the same time, structural disorders appearing in many pathologies are preceded by biological and initial morphological changes. Therefore, information about these changes is very important for diagnostics. The use of the polarisation properties of probe radiation propagating in a sample can increase the specificity of OCT.

This approach was employed in the method of polarisation-sensitive OCT (PSOCT) [10, 12 – 18]. PSOCT can provide important information on the inner structure of biological objects, which cannot be obtained by conventional OCT, for example, on the burn damage depth [12 – 14] and tooth demineralisation [15, 16] and also makes it possible to perform early diagnostics of osteoarthritis [17]. To perform an early diagnostics of cancer, it is necessary to detect reliably an optical signal from the depth 400 – 700 μm, at which a basal membrane is located. To measure reliably the phase characteristics, such as the birefringence of a medium, a sufficiently large signal-to-noise ratio should be provided (no less than 10 – 15 dB), which is difficult to

R.V. Kuranov, V.V. Sapozhnikova, H.M. Shakhova, V.M. Gelikonov, E.V. Zagainova, S.A. Petrova Institute of Applied Physics, Russian Academy of Sciences, ul. Ul'yanova 46, 603950 Nizhnii Novgorod, Russia; e-mail: roman@appl.sci-nnov.ru

Received 18 June 2002
Kvantovaya Elektronika **32** (11) 993 – 998 (2002)
Translated by M.N. Sapozhnikov

achieve for layers at the depth more than 300 – 500 μm [12, 16].

In our previous papers, we considered the possibility of early diagnostics using a variant of PSOCT – the method of cross-polarisation OCT (CPOCT) [10, 19, 20]. A comparison of this method with other PSOCT methods was performed in detail in paper [10]. The CPOCT method is based on the measurement of probe radiation scattered backward by tissues and having orthogonal polarisation compared to that of the incident radiation. This scattering can be determined by the depolarising properties of tissues and by a macroscopic linear birefringence inherent in some tissues [20]. The polarisation of scattered radiation can be determined, for example, by collagens, which form the basis of a stromatic tissue. The localisation and orientation of collagenic fibres can be determined with the help of an additional histological-chemistry analysis. In our opinion, a combined use of histological chemistry and CPOCT provides a better interpretation of the CPOCT data.

The specificity of OCT can be also improved by using it in a combination with the fluorescence spectroscopy (FS) of tissues, which is based on the difference of the spectral parameters of pathologic and healthy regions of the tissue. To increase the intensity of tumour emission, exogenous fluorophores are used or fluorescence sensitisers [for example, 5-aminolevulinic acid (5-ALA)] [21]. The internal application of 5-ALA induces a selective accumulation of endogenous porphyrins in cancerous cells, resulting in a drastic enhancement of the fluorescence intensity of tumours compared to that in a normal tissue, where porphyrins are not accumulated. The fluorescence intensity characterises the amount of porphyrins accumulated in cancerous cells and, hence, the malignancy of the process.

Note, however, that porphyrins are accumulated not only in malignant but also in benign tumours, as well as in proliferous tissues, i.e., in all proliferous cellular populations, which somewhat impairs the diagnostic ability of this method. Therefore, the specificity of FS with respect to the differentiation of inflammatory and oncology processes is low. At the same time, OCT well visualises structural variations in tissues, while FS allows one to estimate the amount of protoporphyrin accumulated in tissues at depths up to 1 – 2 mm. Therefore, a combination of these methods improves the diagnostics of cancerous diseases.

The aim of this paper is to study the possibilities of combined optical methods for diagnostics of neoplastic processes. We propose to extend the possibilities of OCT by using this method in combination with CPOCT and FS.

2. Combined application of conventional OCT and CPOCT

It is known that some structural units of biological objects, for example, the collagens of stromatic tissue, which forms a healthy mucous membrane, can strongly depolarise incident radiation [22]. Pathologic processes of a different nature are characterised by different contents of collagenic fibres and by their different spatial orientation. Therefore, diagnostics of a neoplastic process can be based on a comparative study of the depolarising properties of biological objects. It was shown in paper [20] that a CPOCT image of pathologic tissues is determined by their depolarising properties. Because only pathologic tissues were studied by the CPOCT method, we will neglect below the fact that CPOCT images can be also related to macroscopic linear birefringence in samples. To verify the OCT and CPOCT images, we performed a comparative analysis of biopsy samples obtained from the same place. They were coloured by two different methods: with hematoxylin eosin (for general diagnostics) and using the Van Gison technique for colouring the connective tissue, which is specific with respect to the differentiation of collagenic fibres of connective tissue [23].

The scheme of the experimental setup for the CPOCT study of tissues is shown in Fig. 1. Low-coherence radiation from a superluminescent diode (*1*) is optically combined in a multiplexer (*3*) with radiation from a red diode laser (*2*), which is used to align the system. Then, radiation is delivered, through a Lefevre polarisation controller, to one of the intrinsic axes of an anisotropic 3-dB fibre coupler. A polarisation-retaining fibre is used to deliver radiation of a certain polarisation through the signal and reference arms. When a Faraday rotator (*10*) was absent in the reference arm, a non-depolarised component of backward scattered radiation was detected. In the presence of a 45° Faraday rotator in the reference arm, backward scattered radiation was polarised perpendicular to the incident radiation, so that only the radiation component depolarised by a biological object interfered.

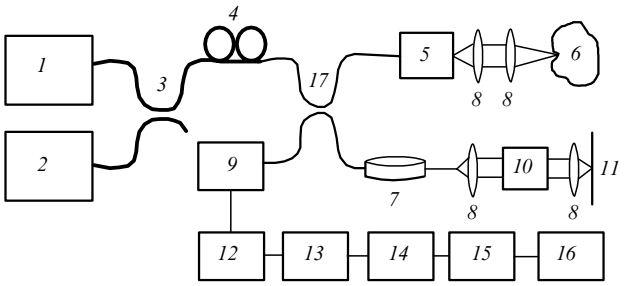

Figure 1. Experimental setup for cross-polarisation OCT: (*1*) superluminescent diode; (*2*) diode laser; (*3*) multiplexer; (*4*) polarisation controller; (*5*) transverse scanner; (*6*) object; (*7*) longitudinal scanner; (*8*) lenses; (*9*) photodiode; (*10*) 45° Faraday rotator; (*11*) highly reflecting mirror; (*12*) selective amplifier; (*13*) logarithmic amplifier; (*14*) amplitude detector; (*15*) analogue-to-digital converter; (*16*) PC; (*17*) 3-dB fibre coupler. An isotropic single-mode fibre is shown by a thick line, and a polarisation-retaining fibre is shown by a thin line.

Note that during the system realignment for obtaining an image in the orthogonal polarisation, the position of a flexible probe was fixed, providing the detection of images of both types for the same region. The realignment time was 30 s. This scheme with an anisotropic fibre was used in a portable instrument with a flexible probe, which is convenient for clinical applications, in particular, endoscopic [10].

Tomograms of the esophagus cancer were obtained *ex vivo* for resected esophagus (no more than 60 min after extirpation). The OCT images of scar changes were obtained *in vivo* upon esophagoscopy. All the experimental studies were performed with permission of a patient and the administration of the N.A. Semashko Nizhnii Novgorod regional hospital.

Fig. 2 shows the results of the study of carcinoma and scar tissue of esophagus. Standard samples of these patho-

logic tissues are barely distinguishable (Fig. 2a) because both tomograms have no structure. Therefore, it is virtually impossible to distinguish cancer from scar changes using conventional OCT. In this case, the diagnostics is performed based on visual observations and histological studies of biopsy materials (Fig. 2c).

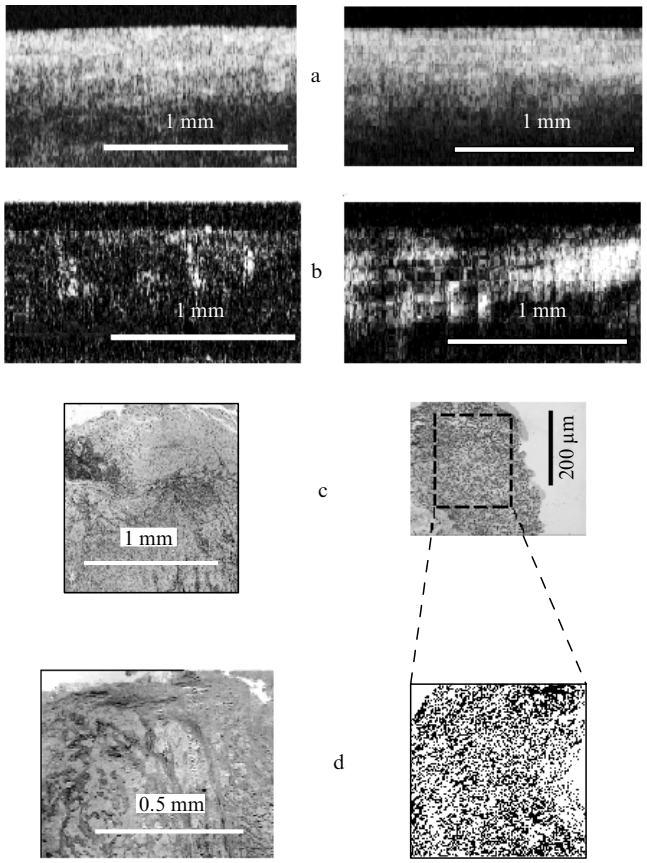

Figure 2. Combined optical diagnostics of the esophagus cancer (at the left) and scar tissue (at the right). (a) Standard OCT image; (b) CPOCT image; (c) colouring with hematoxylin-eosin; and (d) Van Gison colouring.

However, CPOCT images of these two pathologies substantially differ from each other (Fig. 2b). A cancerous tumour almost does not depolarise probe radiation – the signal intensity is lower by 30 dB on average than that for a healthy tissue, which is explained by the loosening of a compact stroma during carcinogenesis. The positions of new unripe collagenic fibres synthesised by the tumour, which have different biochemical properties and optical parameters, can be revealed by colouring the tissue with picrofuchsin (Van Gison colouring), because disordered and unripe collagenic fibres are weaker coloured with picrofuchsin (became pink) compared to fibres of a ripe connective tissue. The collagen of stroma does not ripe completely during carcinogenesis because, simultaneously with the stroma rearrangement during the tumour growth, the preceding collagenic structures are continuously destroyed, being replaced by more separated and unripe fibres.

The histological description of collagenic fibres, which represents elongated individual dark structures (at the left of Fig. 2d), well correlate with the CPOCT images of esophagus cancer, where vertical inclusions of a stronger signal are observed against the background of a very weak signal (at the left of Fig. 2b).

The CPOCT images of the scar tissue of esophagus reveal a significant depolarisation of probe radiation, which exceeds the depolarisation signal from the cancerous tumour by 10 dB on average (at the right of Fig. 2b). In this case, many randomly oriented regions of the intense and weak signals are observed. This is explained by the different nature of formation of the scar tissue compared to the cancerous tissue: the healing of wounds is accompanied by the formation of the granular tissue and by the enhanced synthesis of new collagenic fibres. Indeed, one can see in Fig. 2d (at the right) the alternating darker regions, corresponding to more ripe collagenic fibres, and white and light-grey regions, which corresponds to the accumulations of cells of the granular tissue.

3. Combined application of OCT and fluorescence spectroscopy

It is known that tissues that were subjected to neoplastic changes often have no distinctly visible boundaries with a normal tissue. The boundaries of pathological regions can be determined quite accurately from the OCT images due to the effect of disappearance of a layered structure. The previous studies showed that the boundary of a malignant tumour determined by the OCT method, and verified morphologically, can extend beyond the visible boundary by 3–5 mm on average [24]. Because the oncological process is accompanied not only by structural but also by preceding biochemical changes of the tissue, we decided to perform a comparative analysis of OCT and induced fluorescence spectroscopy with the use of 5-ALA. We carried out experiments with oncogynecological objects (uterine cervix and vulva), which were available to us.

The fluorescence spectra of biological tissues were recorded *in situ* with a LESA-01-BIOSPEK laser setup (BIOSPEK, Moscow) for the fluorescence diagnostics of tumours and control of the photodynamic therapy of cancer [25]. The setup consisted of a 633-nm, 12-mW LGN633-25 BIOSPEK laser and a spectrometer operating in the spectral range from 500 to 900 nm. Laser radiation was delivered through a flexible fibre to an object. The fluorescence of a tissue excited by laser radiation and a part of backward scattered radiation were coupled to the detection part of a fibreoptic catheter and delivered to a unit consisting of a set of optical filters, which were used for scaling the intensity of scattered radiation. Backward scattered laser radiation and fluorescence were analysed with a diffraction polychromator. The emission intensity was detected with a 1024-channel photodiode array in a broad spectral range. The fluorescence spectra were processed using a packet of applied programs.

All the data obtained in experiments were normalised to the maximum of reflection of laser radiation at 633 nm. The fluorescence intensity was characterised by the fluorescence coefficient F_{fl}, which was defined as the ratio of the area S_1 under the fluorescence band of protoporphyrin IX in the range from 675 to 715 nm to the area S_2 under the spectral curve of diffusely scattered laser radiation in region from 620 to 640 nm:

$$F_{\mathrm{fl}} = S_1/S_2. \tag{1}$$

The fluorescence coefficient was measured in real time. Then, we measured the contrast coefficient C_c, defined as the ratio of the fluorescence intensity in the region from 675 to 715 nm to the fluorescence intensity of the environmental healthy tissue.

The coefficient F_{fl} for a healthy tissue was measured at healthy parts of the uterine cervix of a patient. We averaged fluorescence data obtained at least for ten healthy parts of the tissue. Thus, we measured fluorescence coefficients for different uterine cervices, which varied from 0.3 to 0.5 for different females. The contrast coefficient C_c was calculated as the ratio of the fluorescence coefficient for a pathologic part of the tissue ($F_{fl\,i}$, the subscript i corresponding to the part number) to that for the environmental healthy tissue ($F_{fl\,n}$):

$$C_c = F_{fl\,i}/\,F_{fl\,n}. \qquad (2)$$

The contrast coefficient for healthy parts of the tissue is close to unity. Coefficients (1) and (2) measured in experiments allow us to optimise the fluorescence contrast between healthy and pathologic parts of the tissue. The data were processed with a special computer program.

The fluorescence analysis was performed using 5-ALA (Research Institute of Organic Intermediate Products and Dyes, Moscow), which is a predecessor of endogenous porphyrins. Crystalline, freshly prepared 5-ALA was dissolved in 200 ml of water in a dose of 15 mg per 1 kg of the patient weight and was administered per os. Within 2.5 – 3 h after the 5-ALA administration, the OCT and fluorescence data were detected under the colposcopic control. To minimise the effect of false-positive fluorescence related to inflammatory reactions, the patient vulva sanitation was performed using betaine. The mucous membrane was treated directly before the study with a 3 % solution of hydrogen peroxide for cleaning and reducing the background bacterial fluorescence. A standard clinical inspection involved simple and extended colposcopy of uterine cervix. The extended colposcopy was performed using a test with 3 % acetic acid to visualise a changed epithelium and the determination of the visual boundary of a damaged tissue.

We inspected six patients with neoplasia of uterine cervix and vulva (precancer, noninvasive and invasive cancer). To determine the boundaries of a pathologic region, we detected fluorescence and scattering of light for the same parts of the healthy and pathologic tissue successively, beginning from the tumour centre to its periphery, by moving in 1-mm steps to the damage boundary and further, up to a distance of 1 cm from the visual boundary, which was determined colposcopically. Then, we obtained the OCT images of the same region of the tissue. All the measurements were performed in real time. Optical studies were performed for one or two parts of the tissue, but a biopsy material from the tumour centre and its optical boundary was taken only from one of them. The OCT images showing the boundary between the optically structureless tumour tissue and the healthy tissue having a distinct layered structure were obtained from visually healthy parts of uterine cervix at a distance of ~ 2 mm from the colposcopic boundary of damage (2.3 ± 0.75 mm with variations from 1 to 4 mm). The optical boundary was determined from the OCT data as a place where structureless images were transformed into structured ones. The optical fluorescence boundary of the pathologic region was determined as a place where the fluorescence intensity drastically decreased to the value characteristic of the healthy tissue.

OCT allowed us to determine rather accurately the boundaries of the tissue damage (Fig. 3). The tomogram in Fig. 3c distinctly visualises the boundary between the pathologic and healthy epithelium. This allows us to localise accurately the tumour boundary, which is confirmed by the histological analysis of the biopsy material and corresponds morphologically to the hyperneoplasia of epithelium. The fluorescence spectra obtained from the damage centre (Fig. 4) exhibited two typical bands at 675 nm (porphyrins) and 700 nm (protoporphyrin IX). The 675-nm band in the fluorescence spectrum of a healthy tissue is weak, while the 700 – 705-nm band is absent at all.

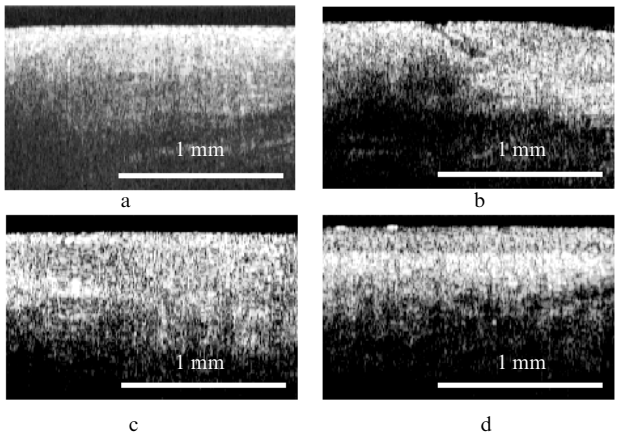

Figure 3. OCT images of uterine cervix: (a) tumour centre; (b) colposcopic boundary between the tumour and a visually normal tissue; (c) OCT boundary between the tumour and a normal tissue (norm is at the left); and (d) the normal uterine cervix tissue.

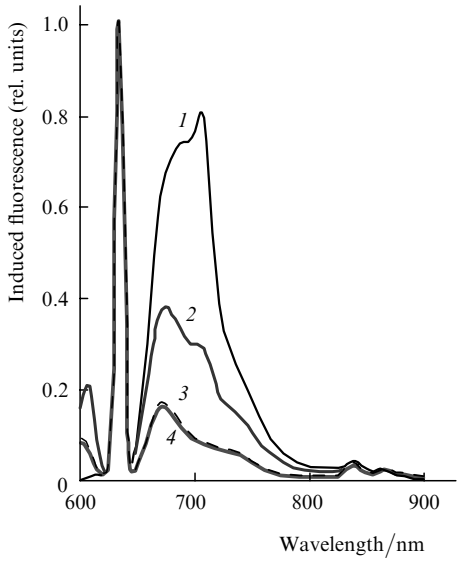

Figure 4. Induced fluorescence spectra of the tumour of a patient V. obtained using 5-ALA from (*1*) the tumour centre, (*2*) the visual boundary between the tumour and normal tissue, (*3*) from the OCT boundary between the tumour and normal tissue, and (*4*) a healthy tissue.

We calculated the fluorescence coefficients F_{fl} for healthy and pathologic tissues of patients. For the healthy tissue, $F_{fl} = 0.3 - 0.5$, while for neoplasia this coefficient varies in a broad range from 1.8 to 5.4. Depending on the stage of a malignant process, the average value of F_{fl} was 3.1 ± 0.99. We also calculated the contrast coefficient C_c. Fig. 5 shows the histogram of the distribution of C_c in the direction from the centre of the damaged tissue to healthy regions. The fluorescence coefficient for protoporphyrin IX decreased to the norm at a distance of 2 mm (2 ± 0.57 mm with variations 1–3 mm) from the colposcopic boundary. In some cases, the fluorescence intensity drastically decreased almost to the norm at a distance of 1–3 mm from the visual boundary. In other cases, upon moving from the centre to periphery, the fluorescence intensity decreased gradually to the level of fluorescence of normal epithelium. In six cases from ten, the fluorescence and OCT boundaries coincided. Biopsy tissue samples taken from these regions confirmed our assumption that the visual boundaries of the damaged tissue in oncological processes do not coincide with optical boundaries. In two cases of histological analysis of a material taken from the colposcopic boundary, we found changes that were similar to those observed at the tumour centre (Fig. 3a). The OCT images of the visual boundary are structureless, which reflects tumour reactions of the tissue. The intensity of fluorescence of this part of the tissue was lower than from the tumour centre; nevertheless, it was considerably greater than the fluorescence intensity of the surrounding healthy tissue (Fig. 4).

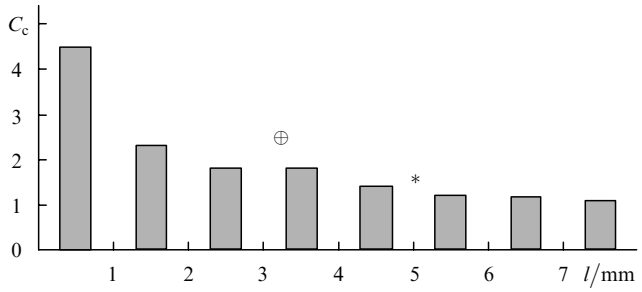

Figure 5. Histogram of the dependence of the fluorescence contrast coefficient C_c on the distance to the tumour centre. Symbols ⊕ and * denote colposcopic and optical (FS + OCT) boundaries of the tumour, respectively.

Therefore, we can conclude that optical boundaries determined by two different methods do not coincide, as a rule, with colposcopic boundaries (in eight cases from ten). However, in two cases of studying exophytic growths, the optical and visual boundaries of tumours coincided, which we explain by the type of growth of these tumours.

4. Discussion

It has been shown in [26] that OCT can be used to reveal structural changes in tissues caused by pathologic processes such as inflammation, tumours, and tumour-like growths. However, conventional OCT is less sensitive to changes in the connective tissue than CPOCT, because the latter method yields additional information on a biological object related to its depolarising properties. While OCT can be compared with a standard morphological analysis in respect of the information content, CPOCT can be considered to some degree as an *in vivo* analogue of the histochemical study. A combined application of conventional OCT and CPOCT can substantially increase the diagnostic ability of the method due to a higher specificity.

Biochemical processes proceeding in tissues during the development of neoplasia can be studied by the method of fluorescence spectroscopy with the use of 5-ALA [27]. However, this method is not specific to neoplasia because the percentage of false results caused by the enhancement of fluorescence during inflammatory processes remains high. A combined application of laser-induced fluorescence and OCT allows us to obtain more detailed information on structural and biochemical changes occurring in tissues.

An advantage of our combined method for detecting tumours over other methods is its low cost and the absence of side effects of laser radiation. We used low-power lasers emitting in the near-IR and visible regions. The radiation is noninvasive and can deeply penetrate into tissues, allowing the diagnostics of hidden tumours with the endophytic type of growth at a depth of 1–2 mm.

Therefore, a combined application of OCT, CPOCT, and fluorescence spectroscopy brings the concept of 'optical biopsy' closer to the realisation. The role of optical biopsy in diagnostics is determined by its ability to reveal the structural and biochemical changes in tissues with high resolution. First of all, this is a sighting biopsy and a precise detection of the linear parameters of tumours, which is important for determining the stage of the process and planning the resection line in organ-retaining operations [28, 29]. These noninvasive, fast-response methods devoid of side effects are attractive for clinical applications and quick diagnostics. Note also that the equipment is comparatively low-cost. All this allows us to hope that optical diagnostic methods will be extensively used in practical medicine.

5. Conclusions

We have shown that CPOCT can provide new information on biochemical changes in the tissue affecting its depolarising properties. It is shown CPOCT in combination with standard OCT can distinguish such pathologies as cancer and scar changes in esophagus. Such diagnostics cannot be performed by conventional OCT only.

A combined application of OCT and fluorescence spectroscopy with the use of 5-ALA makes it possible to determine more accurately the tumour boundary in the tissue. Our study has shown that the optical boundary is located on average 2-mm beyond the visual boundary. The histological studies of the tissue confirmed the non-coincidence of the visual and optical boundaries of a cancerous tumour. We have shown that a combined optical diagnostics of neoplastic processes based on the study of morphological changes by standard OCT and of biochemical changes by CPOCT and fluorescence spectroscopy with the use of 5-ALT is promising for clinical applications.

Acknowledgements. The authors thank E.V. Zagainov and A.N. Denisenko for their help in the obtaining of OCT images under clinical conditions and L.B. Snopova for her help in the interpretation of the results of histological studies.

References

1. Choi B., Barton J.K., Chan E.K., Welch A.J. *Las. Surg. Med.*, **23**, 185 (1998).
2. Farkas D.L., Du C., Fisher G.W., Lau C., Niu W., Wachman E.S., Levenson R.M. *Comput. Med. Imaging Graph.*, **22**, 89 (1998).
3. Manni J. *Biophotonics International*, (1–2), 44 (1996).
4. Messmann H., Kullmann F., Wild T., Knuchel-Clarke R., Ruschoff J., Gross V., Scholmerich J., Holstege A. *Endoscopy*, **30**, 333 (1998).
5. Gelikonov V.M., Gelikonov G.V., Gladkova N.D., Kuranov R.V., Nikulin N.K., Petrova G.A., Pochinko V.V., Pravdenko K.I., Sergeev A.M., Fel'dshtein F.I., Khanin Ya.I., Shabanov D.V. *Pis'ma Zh. Eksp. Teor. Fiz.*, **61**, 149 (1995).
6. Huang D., Wang J., Lin C.P., Shuman J.S., Stinson W.G., Chang W., Hee M.R., Flotte T., Gregory K., Puliafito C.A., Fujimoto J.G. *Science*, **254**, 1178 (1991).
7. Schmitt J.M. *IEEE J. Sel. Top. in Quantum Electron.*, **5**, 1205 (1999).
8. Gladkova N.D., Petrova G.A., Nikulin N.K., Radenska-Lopovok S.G., Snopova L.B., Nasonova V.A., Gelikonov G.V., Gelikonov V.M, Kuranov R.V., Sergeev A.M., Feldchtein F.I. *Skin Research and Technology*, **6**, 6 (2000).
9. Pitris C., Jesser C., Boppart S.A., Stemper D., Brezinski M.E., Fujimoto J.G. *J. Gastroenterol.*, **35**, 87 (2000).
10. Shakhova N.M., Gelikonov V.M., Kamensky V.A., Kuranov R.V., Turchin I.V. *Laser Phys.*, **12**, 617 (2002).
11. Hittinger J.W., Mattozzi M., Myers W.R., Williams M.E., Reeves A.,, Parsons R.L., Haskell R.C., Petersen D.C., Wang R., Medford J.I. *Plant Physiol.*, **123**, 3 (2000).
12. Schoenenberger K., Colston B.W. Jr., Maitland D.J., DaSilva L.B., Everett M.J. *Appl. Opt.*, **37**, 6026 (1998).
13. De Boer J.F., Srinivas S.M., Malekafzali A., Chen Z.P. Nelson J.S. *Opt. Expr.*, **3**, 212 (1998).
14. De Boer J.F., Srinivas S.M., Park B.H., Pham T.H., Chen Z.P., Milner T.E., Nelson J.S. *IEEE J. Sel. Top. Quantum Electron.*, **5**, 1200 (1999).
15. Feldchtein F.I., Gelikonov G.V., Gelikonov V.M., Iksanov R.R., Kuranov R.V., Sergeev A.M., Gladkova N.D., Ourutina M.N., Warren J.A., Reitze D.H. *Opt. Expr.*, **3**, 239 (1998).
16. Baumgartner A., Dichtl S., Hitzenberger C.K., Sattmann H., Robl B., Moritz A., Fercher Z.F., Sperr W. *Caries Research*, **34**, 59 (2000).
17. Drexler W., Stamper D., Jesser C., Li X.D., Pitris C., Saunders K., Martin S., Lodge M.B., Fujimoto J.G., Brezinski M.E. *J. Rheumatol.*, **28**, 1311 (2001).
18. Schmitt J.M., Xiang S.H. *Opt. Lett.*, **23**, 1060 (1998).
19. Kuranov R.V., Gelikonov V.M., Shakhov A.V., Terentyeva A.B., Turchin I.V., Kamensky V.A., in *OSA Biomed. Top. Meeting. OSA Tech. Digest* (Washington: Opt. Soc. of America, 2002) p. 275.
20. Kuranov R.V., Sapozhnikova V.V., Turchin I.V., Zagainova E.V., Gelikonov V.M., Kamensky V.A., Snopova L.B., Prodanetz N.N. *Opt. Expr.*, **10**, 707 (2002).
21. Uspenskii L.V., Kuzin M.I., Loshchenov V.B., Ablitsov Yu.A., Rybin V.K., Loginov L.E., Baryshev M.V., Zavodnov V.I. *Khirurgiya*, (5), 21 (1994).
22. Jacques S.L., Roman J.R., Lee K. *Lasers Sur. Med.*, **26**, 119 (2000).
23. Lilly R. *Patogistologicheskaya tekhnika i prakticheskaya gistokhmiya* (Pathohistological Technique and Practical Histochemistry (Moscow: Mir, 1969) Ch. 15.
24. Shakhova N.M., Kuznetzova I.A., Gladkova N.D., Snopova L.B., Pochinko V.V., Chumakov Yu.P., Gelikonov G.V., Gelikonov V.M., Feldchtein F.I., Kuranov R.V., Sergeev A.M. *Proc. SPIE Int. Soc. Opt. Eng.*, **3251**, 59 (1998).
25. Stratonnikov A.A., Loshchenov V.B., Klimov D.V., et. al. *Proc. SPIE Int. Soc. Opt. Eng.*, **3197**, 119 (1997).
26. Sergeev A.M., Gelikonov V.M., Gelikonov G.V., Felchtein F.I., Gladkova N.D., Shahova N.M., Snopova L.B., Shahov A.V., Kusnetzova I.A., Denisenko A.N., Pochinko V.V., Chumakov Y.P., Strelzova O.S. *Opt. Expr.*, **1**, 432 (1997).
27. Tuchin V.V. *Lazery i volokonnaya optika v biomeditsinskikh issledovaniyakh* (Lasers and Fibre Optics in Biomedical Studies) (Saratov: Saratov State University, 1998).
28. Creasman W.T., Zaino R.J., Major F.J., DiSaia P.J., Hatch K.D., Homesley H.D. *Amer. J. Obstet. Gynecol.*, **178**, 62 (1998).
29. Gonzalez D.I., Zahn C.M., Retzloff M.G., Moore W.F., Kost E.R., Snyder R.R. *Amer. J. Obstet. Gynecol.*, **184**, 315 (2001).